Advanced Motion Correction Methods in PET (Review Article)

Arman Rahmim PhD

Department of Radiology, School of Medicine, Johns Hopkins University, Baltimore MD, USA

(Received 15 September 2005, Revised 2 October 2005, Accepted 10 October 2005)

ABSTRACT

With the arrival of increasingly higher resolution PET systems, small amounts of motion can cause significant blurring in the images, compared to the intrinsic resolutions of the scanners. In this work, we have reviewed advanced correction methods for the three cases of (i) unwanted patient motion, as well as motions due to (ii) cardiac and (iii) respiratory cycles. For the first type of motion (most often studies in PET brain imaging), conventional motion-correction algorithms have relied on extraction of the motion information from the emission data itself. However, the accuracy of motion compensation in this approach is degraded by the noisy nature of the emission data. Subsequently, advanced methods, as reviewed in this work, make use of external real-time measurements of motion. Various image-based and projection-based correction methods have been discussed and compared. The paper also reviews recent and novel applications that perform corrections for cardiac and respiratory motions. Unlike conventional gating schemes, in which the cardiac and respiratory gated frames are independently reconstructed (resulting in noisy images), the reviewed methods are seen to follow a common trend of seeking to produce images of higher quality by making collective use of all the gated frames (and the estimated motion). As an observation, a general theme in motion-correction methods is seen to be the use of increasingly sophisticated software to make use of existing advanced hardware. In this sense, this field is very open to future novel ideas (hardware, and especially software) aimed at improving motion detection, characterization and compensation.

Key Words: *Motion tracking, Motion correction, Cardiac gating, Respiratory gating, 4D Image reconstruction, High resolution PET*

Corresponding author: *Arman Rahmim PhD, Division of Nuclear Medicine, Department of Radiology, School of Medicine, Johns Hopkins University, Baltimore MD 21287, USA,*
E-mail: arahmiml@jhmi.edu

I. INTRODUCTION

Recent developments in 3D positron emission tomography (PET) systems have enabled the spatial resolution to reach the 2-5 mm FWHM (Full-Width-at-Half-Maximum) range. With such improvements in spatial resolution, even small amounts of motion during PET imaging become a *significant* source of resolution degradation. In other words, increased spending on new generation scanners can only be fully justified when appropriate motion correction methods are considered, in order to achieve the true resolution of the scanner. To see this, one may note (1) that the effective resolution of an image Δ_{eff} can be written as:

$$\Delta_{eff} = \left[\Delta_{tomograph}{}^{2} + \Delta_{motion}{}^{2}\right]^{1/2} \quad (1)$$

where $\Delta_{tomograph}$ denotes the intrinsic resolution of the scanner (FWHM), and Δ_{motion} is the FWHM of the distribution of the patient's motion. With $\Delta_{tomograph}$ having become comparable to (and no longer much larger than) Δ_{motion}, it is therefore essential to develop and implement accurate patient motion correction techniques.

One must note that a number of motion correction methods developed for SPECT are *not* applicable to PET. This is because these methods rely on the time-dependence of projections in SPECT, due to rotating head(s), which is not the case in PET imaging. Nevertheless, a number of other methods implemented in SPECT imaging are equally applicable to PET (and vice versa) which we have reviewed in this work.

This paper has been broadly categorized into the review and discussion of advanced correction methods for the three cases of (i) unwanted patient motion, as well as motions due to (ii) cardiac and (iii) respiratory cycles. Most of the existing literature on the first type of motion has been investigated and implemented in *brain* PET imaging, since the last two types of motion (which are dominant in whole-body and cardiac PET imaging) are absent in this case. Section II therefore discusses motion-correction methods in brain PET imaging, followed by discussions of advanced correction methods, in sections III and IV, for cardiac and respiratory cycle motions. These sections first discuss existing hardware instrumentation, followed by a review of advanced motion-correction algorithms which make use of such hardware to achieve motion-compensated PET images. Finally, some important areas of future research are discussed in section V, followed by concluding remarks in section VI.

II. BRAIN PET IMAGING

Unlike cardiac and respiratory-related motions, patient movements in brain imaging are unanimously assumed to be of *rigid* nature (i.e. modeled as translational and/or rotational transformations only). As a typical PET brain imaging session can last hours, it is not reasonable to expect a patient to remain motionless during this time. A number of head restraints are nowadays common, such as thermoplastic masks or neoprene caps, which lower the amount of motion but do not eliminate it. Even with head restraints, typical translations in the range of 5-20 mm and rotations of 1-4^{o} are observed[1], depending on the type of mask and the duration of scan (e.g. see (2,3), and also (1) in which a study of various types of head movements, such as those caused by coughing and leg crossing, has been presented).

Methods to correct for such patient movements were in the past largely based on correction of *interscan* movements. These

1. Largest translation typically occurs along the transaxial-(x) axis, and largest rotation around the axial-(z) axis.

(software-based) methods involved the division of a scan into a number of frames, followed by spatial registration of the reconstructed images using mathematical algorithms (e.g. see (4,5)). Nevertheless, motion correction strategies in emission computed tomography (ECT) that rely exclusively on emission data itself are inadequate for robust clinical usage, since (i) they depend on the quality of the scan data – including noise characteristics – and (ii) they assume the activity distribution does not significantly change within the frames, whereas the frames are chosen *a priori*. Because of these disadvantages, this review focuses on methods using external real-time measurements of motion.

Instrumentation: Aside from electromagnetic systems (which suffer from interference with eddy currents in the metal in the PET gantry) and acoustical devices (whose audible signal can be unacceptable especially for neurological studies), the following motion-tracking instruments can be mentioned:

1) A video-camera-based surveillance system used by Picard and Thompson (6) which used 3 LEDs attached to the head of the patient. The system had two CCD cameras placed on the gantry of the PET scanner.

2) The system used by Goldstein et al. (7) based on opto-electronic position sensitive detectors, which worked by optical triangulation of three miniature (lamp) lights fixed to the patient's head. However, the large space between the cameras (1.25 m) prevents the use of this system in PET scanners with long and narrow gantry holes.

3) The nowadays-popular high-resolution (<0.3mm) POLARIS system (1) which is an infrared (IR) opto-electronic motion tracking device using four IR-reflective spheres (depicted in Fig. 1). The system has the advantages that it is commercially available (<$15,000, Northern Digital Inc., Waterloo, Canada), and that using IR-light[2], it is insensitive to room lighting conditions and takes much less disk space to store the IR-tracker output compared to optical image sequences. However, POLARIS has the disadvantage that the reflective spheres need to be affixed in a precisely known geometry[3], and furthermore, similar to all aforementioned methods, the issue of possible *relative motion between the skin and the skull*, during the scan, remains potentially problematic, making the accuracy of these techniques questionable. It is a topic of growing and great interest to the ECT community to minimize or eliminate the latter problem through innovative methods and/or technology.

Figure 1: The POLARIS system uses four infrared-reflective spheres placed in a precisely known geometry.

Motion-correction algorithms: Assuming accurate measurement of patient movement during the scan, a number of approaches to motion compensation have been proposed:

2. A system with CCD video cameras also sensitive to IR light was used in (8); however the reflectors were affixed to a landmark device that was rigidly attached to the teeth of the subject's upper jaw, which proved to be inconvenient for the patients.

3. A proposed solution to this, as shown in www.tru-scan.com (Tru-Scan Imaging Inc.), is the use of head-sets on top of which a plastic board is attached which can be used to hold the POLARIS spheres in the desired geometry.

1) One method (9,3) involves dividing of detected events into multiple acquisition frames (MAFs). That is, with the use of an external monitoring system, every time the displacement of the patient is measured to be larger than a *specified threshold*, the PET data are saved in a new frame. This is then followed by correction of the individually-reconstructed images of the MAFs, via rotation and translation, to compensate for the measured amount of motion (i.e. this is an *image-driven* approach).

The major limitation of the MAF approach is that by using a high motion threshold, motion *within* the frames are neglected; and lowering the motion threshold can instead result in the acquisition of an *increasing* number of *low-statistic* frames to be reconstructed, especially in the presence of considerable movement. Lack of an adequate number of acquired events in the individual frames can in turn adversely affect the quality of the final reconstructed images, and an increased number of frames will also lead to increased reconstruction times.

2) Another *image-driven* correction method proposed by Menke et al. (8) involves post-processing of the motion-blurred reconstructed images using de-convolution operators (whose shape is determined by the measured motion). Nevertheless, this method has not attracted much attention because even though it is theoretically accurate for noise-less data, (i) the de-convolution process amplifies the noise in the PET data, and (ii) when the movements include significant rotation, spatially-*variant* de-convolution filters need to be employed, which increases the computational costs and can introduce other artifacts (8).

3) A more accurate approach consists of correcting individual lines-of-response (LORs) for motion (10) (this is an *event-driven* approach); i.e. motion correction is performed by transforming the LORs along which the events *are* measured to where they *would* have been measured if the object had not moved (this is shown in Fig. 2 for the example of an octagonal scanner).

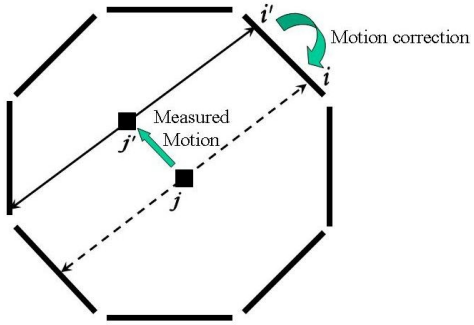

Figure 2: An event that would have been detected along LOR i is detected along LOR i' due to motion. From the measured motion information, one can then transform LOR i' back into LOR i.

The method was elaborated and implemented by Menke et al. (8), and required some hardware modification to achieve on-the-fly motion-corrected LORs. However in that work, due to hardware limitations, the corrected LORs where *not* corrected by normalization factors that corresponded to the *original* detector-pairs (along which the events were detected), and instead the normalization factors for the *transformed* LORs were used. This normalization mismatch has recently been shown to result in artifacts (11).

Alternatively, to solve this problem, one requires a PET scanner either (i) equipped with more specialized hardware to achieve accurate on-the-fly normalization correction followed by LOR-transformation; e.g. see (12), or (ii) capable of acquiring data in list-mode format, so that LOR corrections can be accurately performed post-acquisition; e.g. see (2).

Beyond the purely event-driven approach: The above approach neglects two issues, as raised by Huesman and Qi (13), Rahmim et al.

(14), Thielemans et al. (15) and Buhler et al. (11), which we shall refer to as (issue 1) and (issue 2):

(Issue 1) An event that is normally detected can exit the PET scanner undetected because of motion. This therefore results in a loss of events that would normally have been detected, an effect that is *not* modeled by regular reconstruction methods.

(Issue 2) On the other hand, an event that is normally not detected (i.e. not passing through PET detectors) may be detected because of motion. Therefore, after correction for motion, some detected events may correspond to no actual detector pairs.

These two effects can occur in two ways:

(a) Along the *axial* direction of the scanner, via translation (as shown in Fig. 3) or rotation (not shown); or

(b) Similarly via translation or rotation, along the *transaxial* direction, but only for scanners with *gaps* in between the detectors (an example of this is the High Resolution Research Tomograph - HRRT (16) which has an octagonal design with gaps in-between the heads). This effect is shown in Fig. 4 (for the case of translation).

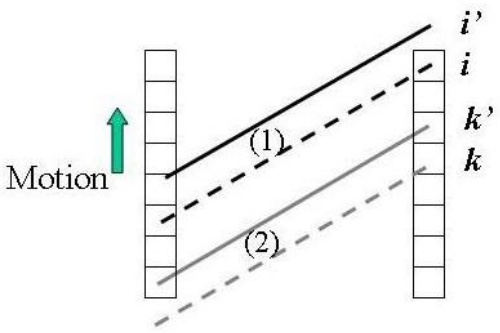

Figure 3: Axial motion can result in (issue 1) LOR i not to be detected (i'), and (issue 2) LOR k, which is normally not detected, to be actually detected (as k). The effect is shown due to translation, but is equally valid for rotation.

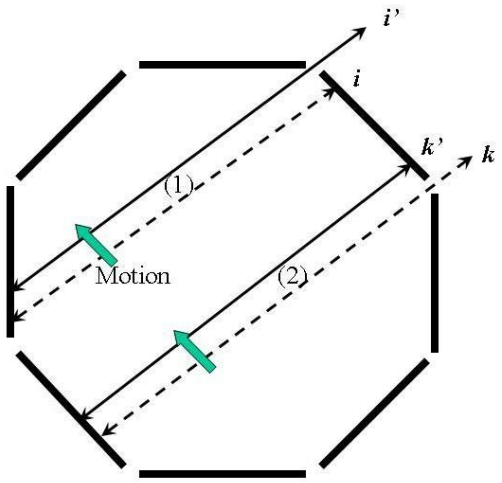

Figure 4: Transaxial motion, for scanners with gaps in between the detector heads, can result in the exact same issues as shown in Fig. 3.

Presence of these two issues can imply the need for a more accurate modeling of the image-data relation into the reconstruction task; otherwise, neglecting the first issue can produce image artifacts, as demonstrated by simulation (15,11) or experimentally (14), and neglecting the LORs obtained in the second case can result in a loss of signal-to-noise ratio (SNR) in the images, as we describe later. Below we review a number of proposed solutions to one or both of these issues:

4) A method suggested by Thielemans et al. (15) addressing (issue 1) involves *scaling* of counts recorded in the motion-corrected sinogram bins in order to correct for the events that were lost due to motion, where the scale factors are computed by averaging of LOR weighting factors using the measured motion information. This can be thought of as a ``motion pre-correction" technique applied to the sinogram bins before the image reconstruction task.

5) The method investigated by Buhler et al. (11), similarly addressing (issue 1), involves using the motion information to divide the total

counts in each motion-corrected sinogram bin by the factor $t_{detectable}/t_{total}$ i.e. the fraction of time each sinogram bin could have been detected by the scanner. Aside from the issue of normalization correction, this method can be shown, though not obvious, to be *equivalent* to the previous method. However, this method pre-corrects the *individual* measured events by related normalization factors, whereas the previous method, which is expected (15) to exhibit less noise, first sums the *un-normalized* motion-corrected LORs and *then* performs normalization correction (by an accurately-calculated overall factor).

The above two methods have two potential difficulties:

(a) They may require consideration of noise enhancement issues, as is done in (15) when *dividing* by *small* scale factors.

(b) *They address (issue 1) but not (issue 2)* because they simply discard motion-corrected events which do not correspond to actual detector elements. It must be noted that neglecting such events should not result in image artifacts (unlike neglecting (issue 1)) since the patient will be still sampled enough by the *existing* detector pairs; however it can result in a loss of SNR in the images since some of the measured signal with useful information is simply discarded.

(iii) A method capable of addressing *both* (issue 1) and (issue 2) has been elaborated by Rahmim et al. (14). The approach is based on modification of the probability system matrix of the iterative expectation-maximization (EM) algorithm. Momentarily neglecting various correction terms (e.g. normalization, attenuation), the regular histogram-mode EM algorithm can be written as

$$f^{new}(j) = \frac{f^{old}(j)}{\sum_{i=1}^{I} p_{ij}} \sum_{i=1}^{I} \frac{p_{ij} n(i)}{\sum_{b=1}^{J} p_{ij} f^{old}(j)} \quad (2)$$

where $f^{old}(j)$ and $f^{new}(j)$ are previous and current activity-distribution image estimates in the iterative EM algorithm, *n(i)* is the number of events detected along an LOR *i*, and p_{ij}, often referred to as the system matrix element, is the probability that an emission from voxel *j* (*j=1…J*) is detected along an LOR *i* (*i=1…I*). For a motion-corrected sinogram (wherein all the events were first corrected for motion before histogramming), the proposed algorithm is able to accurately address issues 1 and 2, and can be written as

$$f^{new}(j) = \frac{f^{old}(j)}{\frac{1}{T}\int_{t=0}^{T}\sum_{i=1}^{I} p_{ij} d_i^t dt} \sum_{i=1}^{I} \frac{p_{ij} n(i)}{\sum_{b=1}^{J} p_{ij} f^{old}(j)} \quad (3)$$

where T is the duration of the scan, and d_i^t is 1 if an LOR *i was* detectable at time *t*, and 0 otherwise. Normalization correction can subsequently be included either (i) as a pre-correction factor (similar to (11)), or (ii) as an intrinsic component of the system matrix element (somewhat similar to (15)). The reader is referred to Ref. (14) for more details.

The above approach has also been proposed (17,14) for list-mode image reconstruction. The list-mode reconstruction approach has a number of general advantages compared to the histogram-mode approach, as elaborated in (18,19); in the context of motion correction, the following two potential advantages can be mentioned:

(a) Events are corrected for motion *during* (and *not* before) the image reconstruction task, which means that the motion-corrected

coordinates can be processed as *continuous* variables, therefore improving the accuracy (whereas time-consuming interpolations may instead be required in histogram-mode methods, as nicely demonstrated by (11), mainly because sinogram bins are not continuous).

(b) Addressing (issue 2) is more convenient in list-mode reconstruction, because in histogram-mode methods, one would have to *extend* the sinogram-space in order to record *all* motion-corrected events (even those that would not have been detected in the absence of motion), whereas in list-mode reconstruction, such events are very easily handled.

Furthermore, Rahmim et al. (14) have also shown that, with appropriate modifications, calculation of the motion-averaging term $\frac{1}{T}\int_{t=0}^{T}\sum_{i=1}^{I} p_{ij}\, d_i^t\, dt$ can be conveniently performed in image-space (instead of projection-space) which for current high-resolution scanners can improve the calculation speed significantly[4] (e.g. the HRRT scanner, with no axial compression i.e. span 1, has ~800M sinogram bins compared to only ~14M voxels in image-space).

III. MOTION DUE TO THE CARDIAC CYCLE

While a spatial resolution of <5 mm is possible with today's PET scanners, the base of the heart moves 9-14 mm towards the apex, and the myocardial walls thicken from approximately 10 mm to over 15 mm between end-diastole and end-systole, as measured from tagged MR images (21). Compared to the intrinsic resolution of today's scanners, cardiac motion can therefore result in significantly blurred images (as seen by Eq. 1). Most common approach in ECT to cardiac cycle motions is *gating* of the data into frames, each representing a particular cardiac phase, as we explain next.

Instrumentation: Cardiac gating is most commonly performed with the aid of electrocardiograph (ECG) devices. By convention, the R-wave (which precedes ventricular contraction) is chosen as the gating signal because it has the greatest amplitude, and is therefore more easily identified in the ECG. In scanners with the list-mode acquisition capability, sorting of the list-mode data into gated frames can be performed *after* the acquisition (e.g. see (22)), whereas in conventional scanners (i.e. with histogram-mode acquisition only), on-the-fly ECG-triggered data acquisition is employed (e.g. see (23)).

Typically, the cardiac cycle is divided into 50-100 ms time frames, and an acquisition ranging from 5-60 minutes is acquired. Most commonly, the obtained cardiac-gated datasets (i.e. cardiac frames) are then *independently* reconstructed (as shown in Fig. 5). This approach is successful in nearly removing the cardiac-motion blurring of the images; *however*, it can produce images which are (much) noisier than a reconstruction of the ungated data, since each gated dataset contains (much) less statistics compared to the entire dataset, and therefore, the clinical utility of this approach is very questionable.

4. In projection-space, Carson et al. (20) have proposed to perform the above calculation over only a randomized subset of the projection-space, in order to produce a fast, practical algorithm; however, the image-space approach proposed in (14) can yield a practical and accurate algorithm with complete (non-randomized) processing of the LORs.

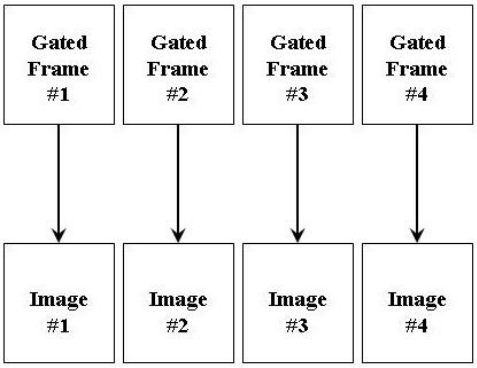

Figure 5: In conventional gated schemes, the gated frames are independently reconstructed (in this example, N = 4 gated frames are shown).

Motion-correction algorithms: The motivation behind advanced correction methods in cardiac imaging is two-fold:

(i) To further improve the quality of cardiac PET images (noise, resolution) so as to enhance identifiably of radiotracer uptake defects in the left ventricle by the clinicians, since regions of decreased radiotracer uptake can be indicative of hibernating or infracted myocardial tissue (24). This is also important when applying quantitative measures of perfusion and metabolic parameters in dynamic compartmental modeling studies (25).

(ii) Measurement of motion itself can be useful for characterizing cardiac function (26). Measures such as ejection fraction and regional wall thickening may be derived from a measure of contractile motion in this way.

In this section, we neglect the problem of cardiac motion due to the respiratory cycle, which is discussed in the next section. Below, we outline five important motion correction approaches which have been proposed in the literature. A common theme amongst these advanced methods is that they seek to move beyond the conventional gated scheme (as was shown in Fig. 5) and instead seek to obtain images which make *collective* use of *all* the gated frames (as depicted in Fig 6). In this way, motion information is extracted from the measured dataset (with the exception of approach 3 which uses modeling), and is used in addition to *all* the gated frames to obtain images of higher quality.

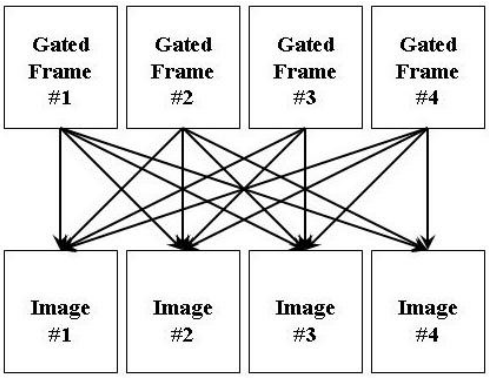

Figure 6: In motion-correction gated schemes, individual images are reconstructed using information from the complete dataset.

The first three outlined works incorporate the measured or modeled motion-information into 4D image reconstruction tasks, while the fourth approach performs the motion estimation and image reconstruction tasks *simultaneously*. Approach 5, on the other hand, performs *image-based* motion correction and summing of 3D reconstructed images. These are elaborated below:

1) In (27,28), Brankov et al. have replaced the uniform-voxel framework with the use of *mesh modeling:* an efficient image description based on non-uniform sampling (*mesh nodes* are placed most densely in image regions having fine detail). This approach is a natural framework for reconstruction of motion image sequences, wherein mesh elements are allowed to deform

over time[5]. Using a gradient-descent search algorithm applied to initial cardiac gated images, the authors are able to determine the *motion field vector* $d_{k\to l}(\mathbf{x})$ mapping a mesh element **x** from the current frame *k* to another frame *l*. The authors have subsequently used the following motion-compensated temporal summation when reconstructing each frame *k*:

$$\hat{f}_k(\mathbf{x}) = \sum_{l=1}^{K} f_l(\mathbf{x} - \mathbf{d}_{k\to l}(\mathbf{x}))$$

(4)

where $f_l(\mathbf{x})$ is the image estimate for the *l*th frame (*k*=1…*K*), and the above expression can be applied as (i) an inter-iteration temporal filter in iterative reconstruction, or as (ii) a post-reconstruction filter[6]. The above summation/filtering step is therefore able to improve the SNR obtained in the cardiac images, since it makes use of information from *other* frames also, when reconstructing a given frame *k*.

Before explaining the remaining methods, we must first explain the concept of *MAP image reconstruction*: A main drawback with the commonly-used expectation maximization (EM) algorithms is that with further iterations the images become increasingly noisy. To tackle this, often a post-reconstruction smoothing filter is used. However, post-filtering, even though lowering the noise, also degrades image resolution. Alternatively, maximum a posteriori probability (MAP) methods[7] have been proposed which, in the 3D-framework, seek to minimize variations between voxels and their neighboring voxels. A particular class of the MAP method (first utilized by Geman and McClure (29) in nuclear medicine), instead of maximizing the Poisson log-likelihood function *L(F)*, as is the case with the regular EM algorithm, instead seek to maximize the MAP function *L(F)-bV(F)*, where *V(F)* is a potential function that decreases in value with less variations for neighboring voxel (*b* is a smoothing parameter set by the user: the higher its value, the greater the amount of smoothing encouraged in the images).

For instance, the so-called 3D-MAP-EM one-step-late (OSL) algorithm, introduced by Green (30) and aimed to maximize the above MAP function, can be written as

$$f^{new}(j) = \frac{f^{old}(j)}{\sum_{i=1}^{I} p_{ij} + b\left.\frac{\partial V(F)}{\partial f_j}\right|_{F=F^{old}}} \sum_{i=1}^{I} \frac{p_{ij} n(i)}{\sum_{b=1}^{J} p_{ij} f^{old}(j)}$$

(5)

and is able to suppress noise more successfully than the regular EM algorithm which can be thought of as a special case of the MAP method with *b*=0. An interesting observation is that the above approach can be extended to a *4D*-MAP algorithm - e.g. see (31,32) - in which one uses a summation of spatial $b_s V_s(F)$ *and* temporal $b_t V_t(F)$ potential functions, in order to encourage smoothing between neighboring voxels in *both* the spatial and temporal directions. We now proceed to explain how motion compensation has been incorporated within the 4D-MAP framework in some of the following works.

2) In (31), Gravier et al. initially reconstruct

5. See http://www.ipl.iit.edu/brankov/MIC02_4D.htm for a very nice dynamic demonstration of this method.

6. Meanwhile, though not shown here, the authors have added another term to the above expression in order to account for brightening of the myocardium as it thickens due to the partial volume effect.

7. This is also referred to as the Baysian method (originally derived from a simple application of Bayes' rule to image reconstruction). It is also, sometimes, referred to as penalized likelihood (PL) image reconstruction.

the gated frames using the fast filtered backprojection (FBP) algorithm, followed by low-pass filtering to reduce the noise. They then use the optical flow approach developed by Horn and Schunck (33) to estimate the motion in-between the reconstructed images. Finally, they use the 4D-MAP-EM-OSL algorithm (4) while defining:

$$V_t(F) = \sum_{k=1}^{K}\sum_{j=1}^{J}\left[f_k(j) - \frac{1}{K-1}\sum_{\substack{l=1 \\ l\neq k}}^{K} f_{l\to k}(j) \right]$$

(6)

where $f_{l\to k}(j)$ denotes the estimated image intensity (in frame *l*) at the location corresponding to voxel *j* of frame *k* (considering the motion). In this way, smoothing is encouraged between voxels in all the frame sequences while taking the motion of the voxels into consideration, and therefore one is able to suppress the noise level that is normally obtained in gated frame images.

3) In the work of Lalush et al. (32,34) in SPECT imaging (which can be similarly applied to PET), a similar 4D-MAP-EM-OSL approach as above has been considered, except that motion is modeled and assumed to be known *a priori* (and *not* measured from initial gated images). The motion vectors are computed by modeling the left ventricular inner and outer walls as ellipsoids that undergo affine transformations (rotation, scaling, and translation) with each frame. The exact form of the potential function is also different in this work. It must be noted, however, that the authors have *not* observed a noticeable degradation when the motion information is simply not included in the 4D-MAP algorithm method (which may have been due to the limited resolution of their scanner). Furthermore, Comparison of the above two approaches is an interesting area of future research, as we discuss in section V.

4) Very commonly in the literature, cardiac motion is estimated *after* reconstructions of gated frames; and in the previously mentioned techniques, this extracted motion information is *then* used in subsequent reconstructions to yield enhanced images (i.e. improved SNRs). In (35) however, Cao et al. have hypothesized that, given the close link between the image reconstruction and motion estimation steps, a *simultaneous* method of estimating the two will be better able to (i) reduce motion blur and compensate for poor SNRs, and to (ii) improve the accuracy of the estimated motion. Their proposed algorithm works by two-step minimization of a *joint* energy functional term (that includes both image likelihood and motion-matching terms). This work has also been extended from a two-frame approach to the complete cardiac cycle in (36). This is a very novel approach, yet its accuracy remains to be demonstrated (e.g. it remains to be verified that the estimated motion matches the actual motion of the heart as measured by, for instance, tagged MR).

5) Klein and Huesman (37) have developed a sophisticated motion-estimation approach which exhibits an impressive knowledge of cardiac anatomy, and makes use of a non-uniform elastic material model to provide accurate estimates of heart motion (from individually reconstructed gated frames). The authors then continue to perform *non-rigid/deformed* summing of the gated images making use of the motion information (i.e. *image-based* motion-compensation). Alternatively, one must note that the estimated motion can instead be directly incorporated into 4D image reconstruction tasks, as explained in the previous works.

IV. MOTION DUE TO THE RESPIRATORY CYCLE

The common approach to the problem of respiratory blurring of PET images has been that of respiratory gating. For instance, respiratory-gated PET has been investigated in imaging of lung cancer to reduce breathing motion artifacts (38,39). In cardiac imaging, combined cardiac-respiratory gating has been implemented in human (40) and animal (22) studies.

Instrumentation: A number of instruments are used for the purpose of measuring respiratory motion:

1) Commonly, a pneumatic bellows is placed around the mid-abdomen of the patient, which monitors variation in pressure in the belt-assembly with stretching of the belt during respiration; e.g. see (41).

2) Another approach (42) involves the Real-Time Position Management (RPM) Respiratory Gating system (Varian Medical Systems), which monitors the motion of the chest wall of the patient by infrared tracking of the vertical position of two reflective markers mounted on a plastic block (stabilized on the patient's abdomen).

3) Livieratos et al. (43) have used an inductive respiration monitor (RespiTrace R250, Studley Data Systems) with a belt around the patient's chest.

4) In animal (mouse) imaging, a respiration sensor (Graseby Medical Limited) has been used by Yang et al. (22) to provide the respiratory signal, being taped to the animal's chest, and connected to a high sensitivity differential pressure transducer.

5) Finally, Beach et al. (41) have used the POLARIS system (described in section II) during cardiac imaging (which has the advantage of monitoring both respiratory *and* unwanted motions). Four infrared reflective markers were placed on an elastic material band, placed around the patient's mid to lower abdomen.

Respiratory-Correlated Dynamic Imaging: In the work by Nehmeh et al. (42), an alternate method which performs respiratory phase-isolation while *not* making use of gating has been implemented (in lung imaging). A radioactive point-source was set on the patient's abdomen, and the data were acquired in very short (e.g. 1-sec) consecutive time frames and were individually reconstructed. In order to capture a specific phase within the breathing cycle, all the images were next analyzed, and those with the point-source at a specific (user-selected) position were then identified, with the corresponding sinograms summed and reconstructed using iterative reconstruction.

This method compared to respiratory gating, while involving significantly more computation, has the advantages that: (i) it does not require tracking hardware to monitor and trace respiratory motion (a benefit for small institutions that do not have a gating system), (ii) it allows reconstruction of PET images at any breathing phase (e.g. phase-matching with the CT image data acquired on PET/CT scanners), and (iii) it is less susceptible to irregular breathing and allows the exclusion of data from irregular breathing cycles. Nevertheless, it has the disadvantage, similar to the conventional gating approach, that less data is used in each reconstruction, and thus the obtained images are more noisy.

Motion-correction algorithms: below we review two proposed advanced methods (one based in projection-space and one in image-space) that seek to obtain images of higher quality compared to images that are otherwise obtained (i.e. by regular respiratory-gating or respiratory-correlated dynamic imaging):

1) The work by Livieratos et al. (43)

performs cardiac imaging by modeling of the respiratory motion of the heart as a *rigid-body* motion, and the parameters for motion correction are obtained from an initial series of respiration-only gated images via edge-tracking of the left ventricle (23). The obtained model is then applied in the form of rigid-body transformations (i.e. translations and rotations) on the list-mode data event-by-event (i.e. motion correction in projection-space). The list-mode approach allows one to make maximal use of the time resolution of list-mode data for interpolation of motion parameters, thus potentially achieving higher accuracy in respiratory motion compensation. After correction of the data for respiratory motion, the authors have proposed to use simple cardiac gating for the rest of the imaging task; however, we note that the more advanced methods presented in the last section can instead be used.

2) Klein et al. (44) have investigated a twelve-parameter affine motion model for 4D-registration of different respiratory gates, which in addition to the six parameters of rotation and translation, allows for three scale and three skew parameters for *non-rigid* motion. However, this approach, which was based in the image-space, was applied to *doubly-gated* cardiac PET sequence as it required images with high SNR for appropriate registration.

Rigid vs. non-rigid modeling of the respiratory motion of the heart: While (43) has claimed the validity of modeling (i.e. approximating) respiratory motion of the heart as rigid-body motion, a number of other works may suggest that non-rigid modeling of respiratory motion of the heart may be beneficial. To start, we note that the non-rigidity of respiratory motion of the heart, which is related to it being pushed and pulled by the diaphragm and other connected tissue, has been investigated using a number of modalities. For instance, the gated CT study in (45) measured on dogs, has recorded an average change of 12% in the total end-diastolic heart volume during forced positive pressure inspiration at 15 cm H_2O. Using echocardiography, similar shape changes have been found in human subjects (46).

Related work by Klein et al. (44) in PET imaging is particularly worth noting: in that work, quantitative measures of respiratory motion of the heart were extracted from ten respiratory-gated patient studies. Translations between end-inspiration and end-expiration were often greater than 10 mm and ranged from 1 to over 20 mm (rigid motion). Moreover, the left ventricle exhibited fairly large compression factors[8] (non-rigid motion) - close to 10% in a number of cases – computed as the product of the three extension factors along the x, y and z directions.

The extension factors were largest along the superior/inferior axis (~5%), which, given the typical 80-100 mm dimension of the left ventricle along this direction, would result in a heart image that would be 4-5 mm too small if motion was assumed simply rigid. Compared to the average 10-mm thickness of the left ventricular wall, this scaling error *may* therefore be considerable. However, with the ECAT EXACT HR scanner, only small improvements were actually observed (44) after performing non-rigid motion modeling, though it is expected that in next-generation (higher-resolution) scanners further improvements may be observed.

V. AREAS OF FUTURE RESEARCH

In this section, I shall attempt to outline few areas of research in motion correction that still

8. The left ventricle was generally largest at inspiration and smallest at end-expiration.

involve open questions, and important areas which demand further inquiries and research:

1) Current motion tracking and correction methods in brain imaging do not address the occurrence of relative motions between the skin and the skull during the scans. This can imply an inaccuracy since motion-tracking lights or reflectors only follow the motion of the surface area to which they are attached (and not necessarily the regions of interest *inside* the brain). It is currently a topic of growing interest to introduce novel methods of characterizing and correcting for this issue.

2) Incorporation of accurate coincidental-accidence (random) and scattered events correction terms, considering patient motion, has received little attention in the past, since normalization/attenuation correction and LOR transformations have been the major issues. In this regard, we note that current random and scatter estimation techniques simply assume a static patient, and therefore, further attention needs to be paid to this topic.

3) In cardiac imaging, it remains an open question as to whether (and in which imaging conditions) it is best to estimate cardiac motion *simultaneously* with the image reconstruction task (as is done in (35)) or *before* application of an advanced image reconstruction algorithm (that makes use of the estimated motion). It also remains an open task to compare the qualities of motion-information obtained from (i) individually-reconstructed cardiac images (e.g. as is done in (31)), or (ii) by means of modeling (e.g. as is done in (32,34)); the comparison is not trivial because the first approach relies on initially *noisy* images while accuracy of the second general approach in the context of *distinct* individual orientations and conditions is in question.

4) In respiratory motion correction, it remains an area of future research to determine whether non-rigid modeling of respiratory motion of the heart has observable advantages compared to rigid modeling.

5) While estimated rigid movements can be easily corrected for in projection-space (by simple translations and rotations of the LORs), it is not straightforward to implement such LOR motion compensations for non-rigid motion. This is, for instance, the reason Klein et al. (44) performed correction of the estimated non-rigid respiratory motion of the heart in image-space. However, projection-space correction methods have the advantage that they make maximal use of the time resolution of data (unlike image-space method which do not assume *any* motion within the gated images). Therefore, it remains an important topic of interest as to whether it is possible/suitable to implement non-rigid motion compensation in projection-space.

6) The principle component analysis (PCA) method elaborated in (47) is a very efficient and natural framework for fast 4D image reconstructions. The method is developed for the motion-free object assumption however, though it has been shown (48) to work very well in reconstructing cardiac image sequences as well (which can indicate that the method is somehow able to intrinsically capture and incorporate motion information). More work is needed in this area to shed light on the potentials of this technique to include accurate motion compensation.

VI. CONCLUSION

In this work, we have reviewed advanced correction methods in PET for the three cases of (i) unwanted patient motion, as well as motions due to (ii) cardiac and (iii) respiratory cycles. Nearly all the work related to the first type of motion has been in brain PET imaging. We have

noted that use of an *external* motion tracking device (and not solely relying on the emission data) is and becoming popular for high resolution PET imaging.

In brain PET imaging, given the rigid nature of motion, it is seen to be more accurate to perform motion corrections in projection-space, instead of image-space, to make maximal use of the time resolution of data. A number of reviewed works have also observed and proposed solutions to complications caused by the motion-based interactions of LORs that are normally detectable and those which are not (e.g. axially out of the field-of-view or passing through detector gaps).

In advanced cardiac and respiratory correction schemes, this paper has observed a general attempt to move beyond the noisy images obtained by cardiac- and respiratory-gated data which are *individually* reconstructed, and instead, advanced techniques are seen to make use of novel motion estimation and image reconstruction applications to obtain images of enhanced quality (improved SNR and resolution). It is therefore observed from the works reviewed in this paper that a general theme has been the use of increasingly sophisticated *software* to make use of existing advanced *hardware*, and that the field of motion correction in high resolution PET is very open to future novel ideas (hardware, and especially software) aimed at improving motion detection, characterization and compensation.

VII. REFERENCES

1. Lopresti BJ, Russo A, Jones WF, Fisher T, Crouch DG, Altenburger DE, Townsend DW. Implementation and Performance of an Optical Motion Tracking System for High Resolution Brain PET Imaging. IEEE Trans Nucl Sci. 1999; 46:2059-2067.
2. Bloomfield PM, Spinks TJ, Reed J, Schnorr L, Westrip AM, Livieratos L, Fulton R, and Jones T. The design and implementation of a motion correction scheme for neurological PET. Phys Med Biol. 2003; 48:959-978.
3. Fulton RR, Meikle SR, Eberl S, Pfeiffer J, Constable CJ. Correction for head movement in positron emission tomography using an optical motion tracking system. IEEE Trans Nucl Sci. 2002; 49:116-123.
4. Woods RP, Cherry SR, Maziotta. A rapid automated algorithm for aligning and reslicing PET images. J Computer Assis Tomog. 1992; 16:620-633.
5. Friston KJ, Ashburner J, Frith CD, Poline JB, Heather JD, Frackowiak RSJ. Spatial registration and normalization of images. Human Brain Mapping 1995; 2:165-189.
6. Picard Y, Thompson CJ. Digitized video subject positioning and surveillance system for PET. IEEE Trans Nucl Sci. 1995; 42:1024-1029.
7. Goldstein SR, Daube-Witherspoon ME, Green MV, Eidsath A. A Head Motion Measurement System Suitable for Emission Computed Tomography. IEEE Trans Med Imag. 1997; 16: 17-27.
8. Menke M, Atkins MS, Buckley KR. Compensation Methods for Head Motion Detected During PET Imaging. IEEE Trans Nucl Sci. 1996; 43(1):310-317.
9. Picard Y and Thompson CJ. Motion correction of PET images using multiple acquisition frames. IEEE Trans Med Imag.

1997; 16:137-144.

10. Daube-Witherspoon ME, Yan YC, Green MV, Carson RE, Kempner KM, Herscovitch P. Correction for motion distortion in PET by dynamic monitoring of patient position (Abstract), J Nucl Med. 1990; 31:816.
11. Buhler P, Just U, Will E, Kotzerke J, van den Hoff J. An Accurate Method for Correction of Head Movement in PET. IEEE Trans Med Imag. 2004; 23(8): 1176-1185.
12. Jones WF, Real-time event stream correction for patient motion in clinical 3-D PET. IEEE Nucl Sci Symp Conf Record. 2001; 4:2062-2064.
13. Qi J, Huesman RH. Correction of Motion in PET using Event-Based Rebinning Method: Pitfall and Solution (Abstract only). J Nucl Med. 2002; 43:146P.
14. Rahmim R, Bloomfield P, Houle S, Lenox M, Michel C, Buckley KR, Ruth TJ, Sossi V. Motion Compensation in Histogram-Mode and List-Mode EM Reconstructions: Beyond the Event-Driven Approach. IEEE Trans Nucl Sci. 2004; 51:2588-2596.
15. Thielemans K, Mustafovic S, Schnorr L. Image Reconstruction of Motion Corrected Sinograms, IEEE Nucl Sci Symp Conf Record. 2003; 4:2401-2406.
16. Wienhard K, Shmand M, et al. The ECAT HRRT: Performance and First Clinical Application of the New High Resolution Research Tomograph. IEEE Trans Nucl Sci. 2002; 49:104-110.
17. Qi J, Huesman RH. List mode reconstruction for PET with motion compensation: a simulation study. Proc. IEEE Inter Symp Biol Imag. 2002; 413-416.
18. Rahmim A, Lenox M, Reader AJ, Michel C, Burbar Z, Ruth TJ, Sossi V. Statistical list-mode image reconstruction for the high resolution research tomograph, Phys Med Biol. 2004; 49:4239-4258.
19. Rahmim A, Cheng JC, Blinder S, Camborde ML, Sossi V. Statistical dynamic image reconstruction in state-of-the-art high resolution PET. Phys Med Biol. 2005; 50:4887-4912.
20. Carson RE, Barker WC, Liow JS, Johnson CA. Design of a motion-compensation OSEM list-mode algorithm for resolution-recovery reconstruction for the HRRT. IEEE Nucl Sci Symp Conf Record. 2003; 5:3281-3285.
21. O'Dell WG, Moore CC, Hunter WC, Zerhouni EA, McVeigh ER. Three-dimensional myocardial deformations: calculation with displacement field fitting to tagged MR images. Radiology. 1995; 195:829-835.
22. Yang YF, Rending S, Siegel S, Newport DF, Cherry SR. Cardiac PET imaging in mice with simultaneous cardiac and respiratory gating. Phys Med Biol. 2005; 50(13):2979-2989.
23. Stegger L. Biedenstein S, Schafers KP, Schober O, Schafers MA. Elastic surface contour detection for the measurement of ejection fraction in myocardial perfusion SPET. Eur J Nucl Med. 2001; 28:48-55.
24. Jadvar H, Strauss HW, Segall GM. SPECT and PET in the evaluation of coronary artery disease. Radiographics. 1999; 19(4):915-926.
25. Hutchins GD, Caraher JM, Raylman RR. A region of interest strategy for minimizing resolution distortions in quantitative myocardial PET studies. J Nucl Med. 1992; 33(6):1243-1250.
26. Nichols K, Lefkowitz D, Faber R, Cooke D, Garcia EV, Yao SS, DePeuy EG, Rozanski A. Echocardiographic validation of gated SPECT ventricular function measurements. J Nucl Med. 2000; 41(8):1308-1314.

27. Brankov JG, Yang Y, Narayanan MV, Wernick MN. Motion-Compensated 4D Processing of Gated SPECT Perfusion Studies. IEEE Nucl Sci Symp Conf Record. 2002; 3: 1380-1384.
28. Brankov, JG, Yang Y, Feng B, King MA, Wernick MN. 4D smoothing of gated SPECT images using a left-ventricle shape model and a deformable mesh. IEEE Nucl Sci Symp Conf Record. 2004; 5:2845-2848.
29. Geman S, McClure D. Baysian image analysis: An application to single photon emission tomography. Proc. Statist. Comput. Sect (Amer. Statist. Assoc.), Washington, DC. 1985; 12-18.
30. Green PJ. Baysian Reconstructions from Emission Tomography Data Using a Modified EM Algorithm. IEEE Trans Med Imag. 1990; 9:84-93.
31. Gravier EJ, Yang Y. Motion-Compensated Reconstruction of Tomographic Image Sequences. IEEE Trans Nucl Sci. 2005; 52:51-56.
32. Lalush DS, Cui L, Tsui BMW. A Priori Motion Models for Four-Dimensional Reconstruction in Gated Cardiac SPECT. IEEE Nucl Sci Symp Conf Record. 1996; 3:1923-1927.
33. Horn BKP, Schunck BG. Determining optical flow. Artif. Intell. 1981; 17:185-203.
34. Lalush DS, Tsui BMW. Block-iterative techniques for fast 4D reconstruction using *a priori* motion models in gated cardiac SPECT. Phys Med Biol. 1998, 43:875-886.
35. Cao Z, Gilland DR, Mair BA, Jaszczak RJ. Three-Dimensional Motion Estimation With Image Reconstruction for Gated Cardiac ECT. IEEE Trans Nucl Sci. 2003; 50(3):384-388.
36. Gilland DR, Mair BA, Sun J. Joint 4D Reconstruction and Motion Estimation in Gated Cardiac ECT. Intern Conf on Fully 3D Image Recon Rad Nucl Med 2005; 303.
37. Klein GJ, Huesman RH. Four-dimensional processing of deformable cardiac PET data. Med Image Anal. 2002; 6:29-46.
38. Boucher L, Rodrigue S, Lecomte R, Benard F. Respiratory gating for 3-dimensional PET of the thorax: feasibility and initial results. J Nucl Med 2004; 45:214-219.
39. Nehmeh SA, Erdi YE, Ling CC, Rosensweig KE, Schoder H, Larson SM, Macapinlac A, Squire OD, Humm JL. Effect of respiratory gating on quantifying PET images of lung cancer. J Nucl Med. 2002; 43:876-881.
40. Klein GJ, Reutter BW, Ho MH, Reed JH, Huesman RH. Real-time system for respiratory-cardiac gating in positron tomography. IEEE Trans Nucl Sci. 1998; 45:2139-2143.
41. Beach DB, Hendrik Pretorius P, Boening G, Bruyant PP, Feng B, Fulton RR, Gennert MA, Nadella S, King MA. Trans Nucl Med. 2004; 51:2693-2698.
42. Nehmeh SA, Erdi YE, Rosenzweig KE, Schoder H, Larson SM, Squire OD, Humm JL. Reduction of Respiratory Motion Artifacts in PET Imaging of Lung Cancer by Respiratory Correlated Dynamic PET: Methodology and Comparison with Respiratory Gated PET. J Nucl Med. 2003; 44:1644-1648.
43. Livieratos L, Stegger L, Bloomfield PM, Schafers K, Bailey DL, Camici PG. Rigid-body transformation of list-mode projection data for respiratory motion correction in cardiac PET. Phys Med Biol. 2005; 50:3313-3322.
44. Klein GJ, Reutter BW, Huesman RH. Four-Dimensional Affine Registration Models for Respiratory-Gated PET. IEEE Trans Nucl Sci. 2001; 48:756-760.

45. Hoffman EA, Ritman EL. Heart-Lung Interaction: Effect on regional lung air content and total heart volume. Ann Biomed Eng. 1987; 15:241-257.
46. Anderson K, Vik-Mo H. Effects of spontaneous respiration on left ventricular function assessed by echocardiography. Circulatin. 1984; 69:874-879.
47. Wernick MN, Infusino EJ, Milosevic M. Fast Spatio-Temporal Image Reconstruction for Dynamic PET. IEEE Trans Med Imag. 1999; 18:185-195.
48. Narayanan VM, King MA, Soares E, Byrne C, Pretorius H, Wernick MN. Application of the Karhunen-Loeve transform to 4D reconstruction of gated cardiac SPECT images. IEEE Nucl Sci Symp Conf Record. 1999; 46:1001-1008.